PAPER • OPEN ACCESS

An engineering modification to the blade element momentum method for floating wind turbines

To cite this article: Simone Mancini et al 2022 J. Phys.: Conf. Ser. 2265 042017

View the article online for updates and enhancements.

You may also like

- Comparison of aerodynamic planform optimization of non-planar rotors using blade element momentum method and a vortex cylinder model
 Ang Li, Mac Gaunaa, Kenneth Lønbæk et
- A multibody approach for 6-DOF flight dynamics and stability analysis of the hawkmoth Manduca sexta
 Joong-Kwan Kim and Jae-Hung Han
- 3D printed self-propelled composite floaters
 Soheila Shabaniverki, Antonio Alvarez-Valdivia and Jaime J. Juárez



ECS Membership = Connection

ECS membership connects you to the electrochemical community:

- Facilitate your research and discovery through ECS meetings which convene scientists from around the world;
- Access professional support through your lifetime career:
- Open up mentorship opportunities across the stages of your career;
- Build relationships that nurture partnership, teamwork—and success!

Join ECS!

Visit electrochem.org/join



2265 (2022) 042017

doi:10.1088/1742-6596/2265/4/042017

An engineering modification to the blade element momentum method for floating wind turbines

Simone Mancini, Koen Boorsma, Marco Caboni, Koen Hermans and Feike Savenije

TNO Wind Energy, Westerduinweg 3, 1755LE Petten, the Netherlands

E-mail: simone.mancini@tno.nl

Abstract. The design of next-generation offshore wind rotors for floating applications carries large uncertainties that make it harder to bring costs down. A significant share of this uncertainty is associated with the use of Blade Element Momentum (BEM) methods to run aeroelastic design and loadcase calculations, because the assumptions underlying the momentum theory are violated by the floater motion. This work presents an engineering method for BEM that allows to model generic floater motions and improves the aerodynamic modelling of floating wind turbines. The new model overcomes the challenge of estimating the apparent wind caused by the platform motion in a simple way, which proves to be very effective for rigid aerodynamic simulations. To verify its impact, BEM results with and without the proposed correction are compared to high-fidelity free vortex wake simulations, imposing the same harmonic motion first to the pitch and then to the yaw degree of freedom of the platform. While little differences are found for the yaw motion, the new floating model clearly improves predictions for the platform pitch case in terms of both aerodynamic loads and induction, finding a very good match with the high-fidelity results. An analysis of the verification data provides new valuable insights on the effect of these motions on aerodynamic loads and performance of a floating wind turbine.

1. Introduction

Floating Offshore Wind Turbines (FOWT) are approaching commercialization [1], yet it is still unclear whether standard tools, developed and validated for bottom-fixed applications, can be relied upon in their design. Indeed, the large floater motions violate the steady-state assumption underlying the momentum theory, shedding serious concerns on the accuracy of those Blade Element Momentum (BEM) methods that form the backbone of most state-of-the-art aeroelastic design codes [2]. This increases the risks associated with the design of next-generation offshore turbines, hampering those cost reductions that would make floating wind energy competitive.

The aerodynamic modelling was recently classified among the major technical challenges concerning the aerodynamics of FOWTs [3]. This is a result of a significantly larger share of unsteadiness in the rotor's operating conditions when comparing a floating turbine to a bottom-fixed design, since the movement of the buoyant platform along its rigid Degrees of Freedom (DoF, figure 1) affects the aerodynamics of both the wake and the airfoils [4].

The effects of floater motions on the aerodynamic performance of FOWTs have been studied by several authors, and an extensive overview of the available literature can be found in [3]. While high-fidelity vortex or Computational Fluid Dynamics (CFD) methods are generally deemed accurate in modelling floating turbines in standard operating conditions, there is not a general

Content from this work may be used under the terms of the Creative Commons Attribution 3.0 licence. Any further distribution of this work must maintain attribution to the author(s) and the title of the work, journal citation and DOI.

2265 (2022) 042017

doi:10.1088/1742-6596/2265/4/042017

consensus about the quality of BEM results (e.g. [5, 6, 7, 8, 9]). Some studies (e.g. [10, 11]) found that the moving platform could trigger the inception of Turbulent Wake State (TWS), or even cause the rotor to operate in a propeller or vortex ring state. However, these conclusions were recently challenged in [12], arguing that the floater motion only affects the instantaneous loading of the rotor without altering the state of the streamtube. In the same work, a new dynamic inflow model for BEM was proposed to model the induced velocity variations caused by a harmonic surge motion (figure 1). The verification against higher fidelity actuator disc models showed promising results, but the engineering model's validity remained limited to the surge motion case.

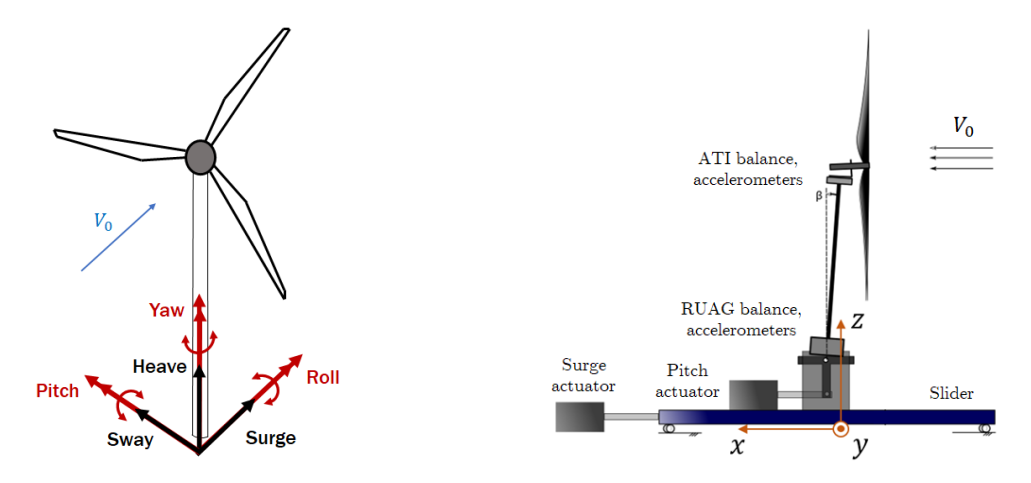


Figure 1. The degrees of freedom of a floating platform.

Figure 2. UNAFLOW experimental set-up sketch.

This work proposes another engineering approach, allowing to model motions along every platform DoF while complying with the recommendations provided in [12]. The model is a generalisation of the approach devised by TNO within project UNAFLOW, in which wind tunnel tests at rotor and airfoil levels were carried out to characterize the aerodynamic response of a FOWT to surge motions and validate numerical models [8]. The main BEM modelling challenges identified were how to distinguish motions induced by floater displacements from standard structural deformations, and how to deal with the non-uniform apparent wind induced by platform rotations [13]. While the first point requires further study on coupled aero-hydro-elastic models, rotations have been successfully modelled in this work.

The goal of this paper is to present the new floating wind model for BEM, with its advantages and limitations. A subset of results from the large verification campaign conducted with a high-fidelity Free Vortex Wake (FVW) code is also presented, providing valuable insights on the effect of harmonic pitch and yaw motions on aerodynamic loads and performance of a FOWT.

2. Models description

This section describes the numerical models that have been used to obtain the results shown in Section 3. The FVW and the standard BEM models are introduced in Section 2.1, while Section 2.2 describes the new model for BEM, and Section 2.3 presents the case study with the main simulation settings.

2.1. TNO AeroModule: AWSM and standard BEM formulation

AeroModule (AM) [14] is a library of aerodynamic solvers, originally developed by ECN (now TNO), which translates decades of wind turbine aerodynamic modelling experience into a state-

2265 (2022) 042017

doi:10.1088/1742-6596/2265/4/042017

of-the-art lifting line tool. The code benefits from a long validation and verification history (e.g. [15, 16, 17, 18]), and it can be used either in standalone mode for aerodynamic calculations on rigid turbines or coupled to an aeroelastic software for loadcase calculations.

Two aerodynamic models are currently implemented in AM: a BEM method; and a higher-fidelity FVW code known as AWSM [19]. Both models rely on the same lookup tables to evaluate the sectional airfoil characteristics, sharing also several sub-models for dynamic stall, 3D airfoil effects, inflow modelling, and tower influence. This allows the use of a single input file for both models, guaranteeing fair and consistent comparisons.

AWSM models the wake creating a lattice of shed and trailed vortex elements that convect from the blades at each time step according to the local wind speed and induced velocity. When modelling a FOWT, besides the airfoil relative wind speed, the platform motion affects the locations where vortices are shed, therefore no special corrections are needed, and all wake-related phenomena (e.g. dynamic inflow, skewed wake) are intrinsically modelled.

Conversely, the BEM method grounds on the momentum theory requiring engineering submodels to account for unsteady or non-uniform wake effects [20]. In its standard formulation, the following momentum equations are solved at every time step and for each blade element to find the annulus induced velocities:

$$\begin{cases}
2\rho A_{ann} u_i U_{Tr} = N_b F_x \\
2\rho r A_{ann} v_i U_{Tr} = -N_b M_x
\end{cases}$$
(1)

with ρ being the air density, A_{ann} the annulus area, r the local radius, u_i the annulus axial induced velocity (along x in rotor plane reference system [21]), v_i the annulus tangential induced velocity (along y in rotor plane reference system), U_{Tr} the transport velocity, N_b the number of blades, F_x the local axial force (in rotor plane reference system), and M_x the local moment with respect to the x axis of the rotor plane reference system.

In AM's BEM the transport velocity, which in the simple axisymmetric case writes $U_{Tr} = V_0 - u_i$ (with V_0 being the free-stream wind velocity), depends on the wind speed and effective yaw angle (Ψ_{eff}) as:

$$U_{Tr} = \sqrt{(||\vec{V}_0|| \cos(\Psi_{eff}) - u_i)^2 + (||\vec{V}_0|| \sin(\Psi_{eff}))^2}$$
 (2)

with $||\vec{V}_0||$ being the norm of the wind velocity vector representative of the annulus [17]. The effective yaw angle combines the rotor yaw and tilt angles relative to the inflow in order to characterize the wake skewness. It is evaluated as follows:

$$\Psi_{eff} = \arctan\left(\sqrt{\tan^2(\Psi_{struc} - \Psi_{wind}) + \tan^2(\gamma_{struc} + \gamma_{wind})}\right)$$
 (3)

with Ψ_{struc} and γ_{struc} being the instantaneous geometric yaw and tilt angles of the rotor plane, whereas Ψ_{wind} and γ_{wind} are the yaw and tilt angles of the rotor average wind velocity vector:

$$\Psi_{wind} = \arctan\left(\frac{\overline{\vec{V}_0} \cdot \vec{j}_{ISYS}}{\overline{\vec{V}_0} \cdot \vec{i}_{ISYS}}\right); \tag{4}$$

$$\gamma_{wind} = \arctan\left(\frac{\vec{V_0} \cdot \vec{k}_{ISYS}}{\vec{V_0} \cdot \vec{i}_{ISYS}}\right); \tag{5}$$

with \bar{j}_{ISYS} , and \bar{k}_{ISYS} being the unit vectors of the x, y, and z coordinates of the ISYS reference frame [21].

2265 (2022) 042017

doi:10.1088/1742-6596/2265/4/042017

The local aerodynamic forces (F_x and M_x in eq. 1) are calculated according to the blade element theory [22], as a function of the local induced velocities including both Prandtl and skewed wake corrections [23, 20], the relative wind speed, and the airfoil characteristics. When a floating turbine is considered, F_x and M_x are the only terms affected by the platform motion because of their dependency on the airfoil relative wind speed.

Note that, for the sake of simplicity, the ECN dynamic inflow term [20] has not been included as it is not affected by the new model described in Section 2.2. Moreover, the equations in (1) are only used until a user-specified induction threshold is reached, and a linear relation for the TWS is used thereafter. The threshold is expressed in terms of the annulus axial induction factor (a) defined as follows:

$$a = \frac{u_i}{\vec{V}_0 \cdot \vec{i}_{RP}} \tag{6}$$

with \vec{i}_{RP} being the unit vector of the x direction of the rotor plane reference system.

2.2. TNO's BEM engineering model for floating wind

In project UNAFLOW, Boorsma and Caboni [13] observed that the apparent wind effect resulting from a surge motion was dominant with respect to that of the rotor moving in and out of its own wake. This evidence was found comparing two AWSM simulations that gave very similar results: one with a harmonic surge motion imposed to the platform; the other with a steady rotor and a sinusoidally varying inflow that replicated the apparent wind velocity introduced by the surge motion in the first simulation. For the first case, the standard BEM predictions were clearly off with respect to the AWSM results. Therefore a special BEM formulation was devised, taking into account the so-called "platform wind" (i.e. the apparent wind velocity introduced by the platform motion) in the momentum part of eq. 1. This was achieved by including the translational velocity of the tower base in the expression of U_{Tr} (eq. 2). The BEM results obtained with the new approach showed a great agreement with both experiments and higher fidelity codes for all the harmonic surge tests considered [8].

The main interpretation was that including the platform wind in the momentum part of the equations allowed to take into account the additional energy exchanged because of floater motions. Indeed, the large displacements that occur cause aerodynamic and hydrodynamic forces to do significant work on the system. And this affects the energy available for the rotor to extract, somewhat similar to a wind speed variation. For example, if the rotor is pushed upwind by the sea waves with a certain velocity the energy available in each annulus would be augmented as a result of hydrodynamic forces.

An important remark needs to be made, however: floater motions are not equivalent to wind speed variations and the TNO approach is purely empirical, with momentum equations being still written in the inertial reference frame of the rotor plane. Therefore this approach, just like the ECN dynamic inflow model, empirically modifies the equations aiming to extend the applicability of BEM to those conditions where classical momentum theory assumptions are violated. This fully qualifies the TNO approach for BEM as a new "engineering" model [24].

Following the success with surge motions, the model validity has been extended to generic platform motions. While the extension to heave and sway (fig. 1) was straightforward, modelling the rotational motions required more changes, since platform rotations induce non-uniform apparent wind velocities throughout the rotor plane.

To derive the platform wind velocity at a generic point from the translation and rotation of the tower base, a rigid body motion has been assumed:

$$\vec{U}_{Pltfm}(P) = \dot{\vec{x}}_B + \vec{\Omega}_B \times \vec{BP} \tag{7}$$

with $\vec{U}_{Pltfm}(P)$ being the platform wind velocity (i.e. the apparent wind velocity induced by the platform motion) at the generic point in space P, $\dot{\vec{x}}_B$ the tower base velocity vector, $\vec{\Omega}_B$ the

2265 (2022) 042017

doi:10.1088/1742-6596/2265/4/042017

tower base rotational speed vector, and \vec{BP} the oriented segment going from the tower base to the generic point P.

The platform wind allows defining an effective wind velocity vector (\vec{V}^*) as:

$$\vec{V}^* = \vec{V}_0 - \vec{U}_{Pltfm} . \tag{8}$$

By replacing $\overline{\vec{V}_0}$ in eq. 4 and 5 with the rotor average effective wind velocity vector $\overline{\vec{V}^*}$, new values for the yaw and tilt angles of the rotor average wind $(\Psi^*_{wind} \text{ and } \gamma^*_{wind})$ are calculated. Inserting them in eq. 3 leads to a new effective yaw angle (Ψ^*_{eff}) , which is used to evaluate both the skewed wake correction [25] and, together with \vec{V}^* , the new transport velocity (U^*_{Tr}) as:

$$U_{Tr}^* = \sqrt{(||\vec{V}^*||\cos(\Psi_{eff}^*) - u_i)^2 + (||\vec{V}^*||\sin(\Psi_{eff}^*))^2}$$
(9)

Obviously when the tower base is fixed the floating model coincides with the standard BEM formulation. Note that including the platform wind in the expression of $U_{T_r}^*$ does not affect the axial induction factor definition, which remains only a function of streamtube properties (eq. 6) in compliance with the recommendations provided in [12].

2.3. Case study

To verify the new model performance its results have been compared to those obtained with both AWSM and the standard BEM formulation. The scaled model of the DTU10MW reference turbine tested in UNAFLOW has been considered [8, 26], hoping to compare with future experimental measurements. The same rigid turbine description and airfoil data prescribed in the IEA Task 30 (OC6) have been used to maximize the reproducibility of the results.

All simulations considered rated conditions with fixed rotor speed $(n = 240 \, rpm)$ and blade pitch $(\theta = 0^{o})$, and a constant uniform inflow velocity of $4 \, m/s$ (in model scale [8]), using a $5 \, ms$ time step. The ECN model for dynamic inflow [20] has been used in all BEM simulations, whereas Snel's first order dynamic stall method [27] has been used for both BEM and AWSM to maximize consistency. The AWSM simulations featured three diameters of wake length, two of which with free convection. The tower influence has been neglected in all simulations.

Mono-harmonic motions have been prescribed to each platform DoF individually. In all simulations the mean turbine position featured a static platform pitch angle of -5^o like in UNAFLOW wind tunnel tests (fig. 2). In order to highlight the impact of the new BEM model, the results are shown for a relatively slow motion frequency (0.25Hz) and quite a large amplitude $(5.1^o$ for the rotational motions). While being representative of real floater motions (in model scale), these have been chosen large enough to affect the different model predictions, but slow enough to limit unsteady effects at both airfoil and rotor levels.

3. Results

This section shows a small but representative subset of the verification results obtained, first focusing on harmonic platform pitch (Section 3.1), and then on yaw (Section 3.2). Both are very interesting cases for verification because, being rotations, they induce a non-uniform apparent wind velocity throughout the rotor plane, which is a challenge for BEM codes. Furthermore, as harmonic motions are considered, a slight dynamic wake skewing occurs since the rotor-inflow alignment changes within a period. This is also a challenge for the new BEM model because it needs to work properly in combination with the skewed wake correction.

The kinematic effects of pitch and yaw are also quite different. While a yawing floater induces limited platform wind velocities, a similar pitch motion strongly affects the apparent wind because of the long lever arm provided by the tower. Here it is reminded that the same sinusoidal signal (with an amplitude of 5.1^{o} and a frequency of 0.25Hz) has been used to prescribe the pitch and the yaw motions individually, always starting from a static platform pitch of -5^{o} .

2265 (2022) 042017

doi:10.1088/1742-6596/2265/4/042017

3.1. Harmonic platform pitch

The main results of the platform pitch case are summarized in fig. 3. The first two plots (3a and 3b) show the time histories of the integral rotor thrust and aerodynamic power for two motion periods. The quantities have been normalised with respect to their average values in order to remove the small static discrepancies that characterize BEM and AWSM results (due to the different wake modelling). This also helps get a quick sense of how severe the observed variations are. The benefit of the floating BEM model is rather clear in both plots. Compared to AWSM, the standard BEM implementation appears to underestimate the oscillation amplitudes featuring a slight phase shift too. The new formulation (labelled "PltfmWind") matches the phase almost perfectly instead, with just a minor amplitude overestimation. These results witness the huge impact that a pitching platform has on performance [28], with the thrust force varying of about $\pm 5\%$ of the steady turbine value, and the power reaching as high as $\pm 20\%$.

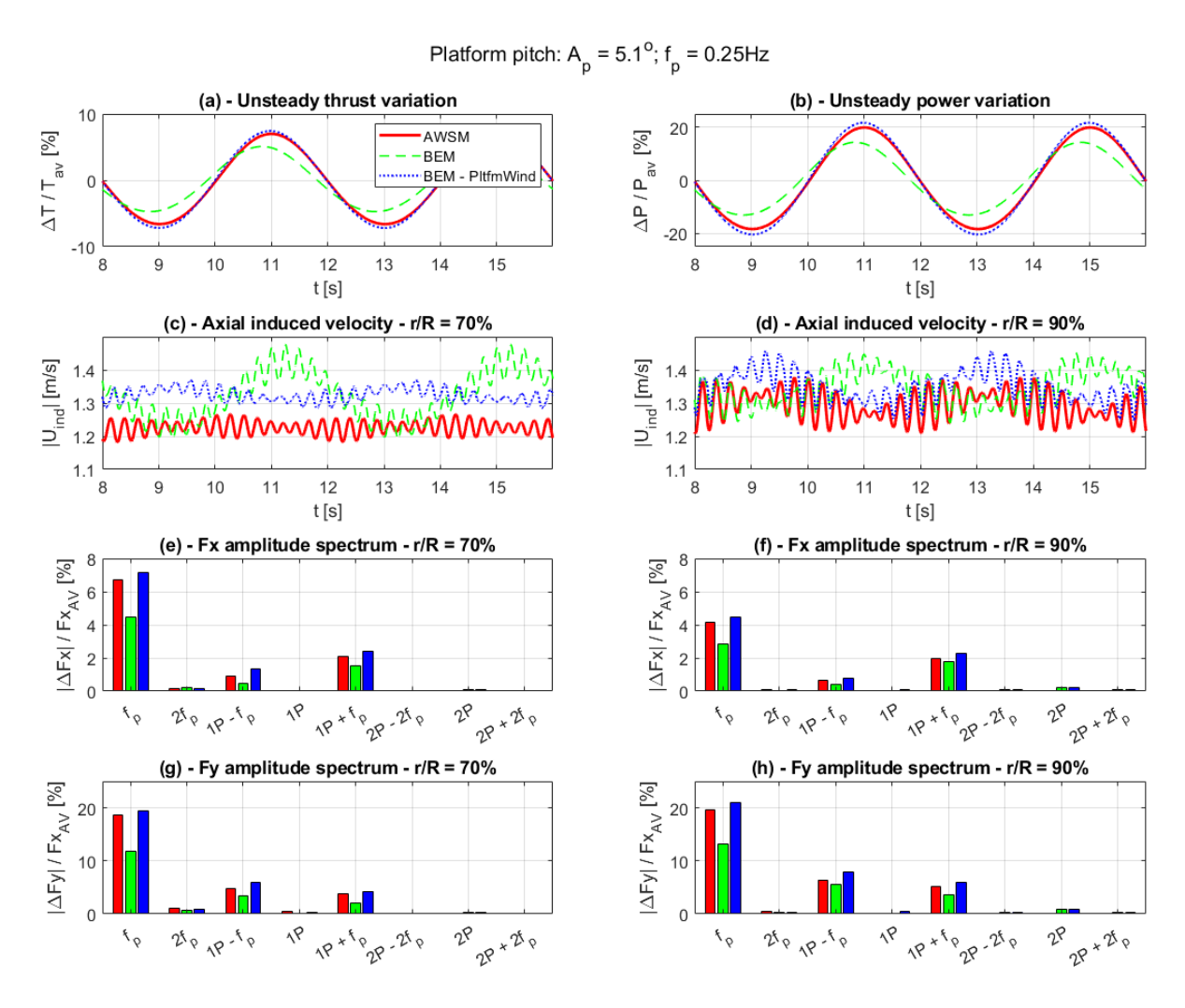


Figure 3. Platform pitch motion figures: (a) integral aerodynamic thrust variation for two pitch cycles; (b) rotor aerodynamic power variation for two pitch cycles; (c) axial induced velocity variation at 70% span for two pitch cycles; (d) Axial induced velocity variation at 90% span for two pitch cycles; (e) amplitude spectrum of the axial unit force at 70% span; (f) amplitude spectrum of the axial unit force at 90% span; (g) amplitude spectrum of the tangential unit force at 90% span.

2265 (2022) 042017

doi:10.1088/1742-6596/2265/4/042017

More insight on the source of discrepancies in the performance plots is provided by the axial induced velocity time histories at 70% and 90% of the span (fig. 3c and 3d). Note that the axial direction refers to the rotor plane reference system, which is inertial but follows the instantaneous orientation of the rotor plane. These two blade stations give an interesting example of how the floating model affects BEM induction values. Though multiple harmonics are present, most of the improvement concerns amplitude and phase of the pitch motion frequency component. This is particularly evident at 70% of the span (fig. 3c), where the standard BEM model overestimates the induced velocity variation amplitude compared to the AWSM results, showing a significant phase shift as well. The amplitude overestimation is likely responsible for the lower integral load variations seen in fig. 3a and 3b. Despite the improvements achieved with the floating sub-model, small discrepancies still separate BEM and AWSM predictions due to the different wake modelling that mainly affects the mean induction values and the skewed wake harmonics.

At last, fig. 3e and 3f show the amplitude spectra of the local axial unit force at the same blade stations. Similar plots for the tangential unit force are reported in fig. 3g and 3h. The spectra have been obtained via the fast Fourier transform with a frequency resolution of $0.125\,Hz$. As for the integral loads, the signals have been normalised by their mean values. Three main remarks can be made observing these graphs:

- (i) Due to the tower lever arm, the main load harmonic occurs at the motion frequency (f_{pitch}) , resulting in $\sim 5\%$ axial and $\sim 20\%$ tangential force oscillation amplitudes.
- (ii) Significant peaks (up to 2% for the axial sectional force, >5% for the torque-generating one) are found at $1P \pm f_{pitch}$ and they are attributed to skewed wake effects that do not appear in the integral quantities because they are compensated among the different blades due to the rotor symmetry. The $1P + f_{pitch}$ appears to be more significant than the $1P f_{pitch}$ for the axial force, whereas both are above 5% in the tangential force spectrum. These harmonics might be detrimental for the blade's fatigue life because they occur at much higher frequencies than the floater motion and they might excite unexpected eigenmodes of the system. For example, the tangential force peak at $1P + f_{pitch}$ could come dangerously close to the frequency of the first edgewise bending mode, which is often poorly damped.
- (iii) The proposed floating model (i.e. 'BEM PltfmWind') has a slight tendency to overestimate the load peaks, whereas the standard BEM implementation underestimates them since the larger induction fluctuations predicted damp the relative wind speed variations. This underestimation is especially severe for the platform motion harmonic.

3.2. Harmonic platform yaw

Similar figures have been generated for the yaw motion case (fig. 4). Differences between the two BEM formulations are less evident than in the pitch case, and the agreement with AWSM appears quite good in general. The aerodynamic performance plots (fig. 4a and 4b) show hardly any difference. However, they indicate that equal rotations around the pitch and the yaw axis have a very different impact on the aerodynamic performance of a FOWT, with thrust and power variations induced by yaw being one order of magnitude smaller than those induced by pitch, confirming what was found in [28]. Furthermore, unlike the pitch motion case, yaw-induced oscillations manifest themselves at twice the motion frequency.

The induced velocity plots (fig. 4c and 4d) show some effects of the floating BEM model that seems to slightly improve induction tracking, especially in terms of phase of the harmonic at twice the motion frequency $(2f_{yaw})$. Looking at the amplitude spectra of the axial (fig. 4e and 4f) and tangential (fig. 4g and 4h) unit forces, it is interesting to see how the signals are dominated by the skewed wake harmonics that are extremely similar to those observed in the pitch results. Here the different plot scales even allow spotting some minor peaks occurring at 2P and $2P \pm 2f_{yaw}$ that are barely present in AWSM results and are a bit overestimated by both

2265 (2022) 042017

doi:10.1088/1742-6596/2265/4/042017

BEM formulations due to the skewed wake correction. As for the pitch, all these high-frequency components are absent from the integral performance plots. Once again the floating model leads to slight overestimations, while the standard BEM formulation is generally underestimating.

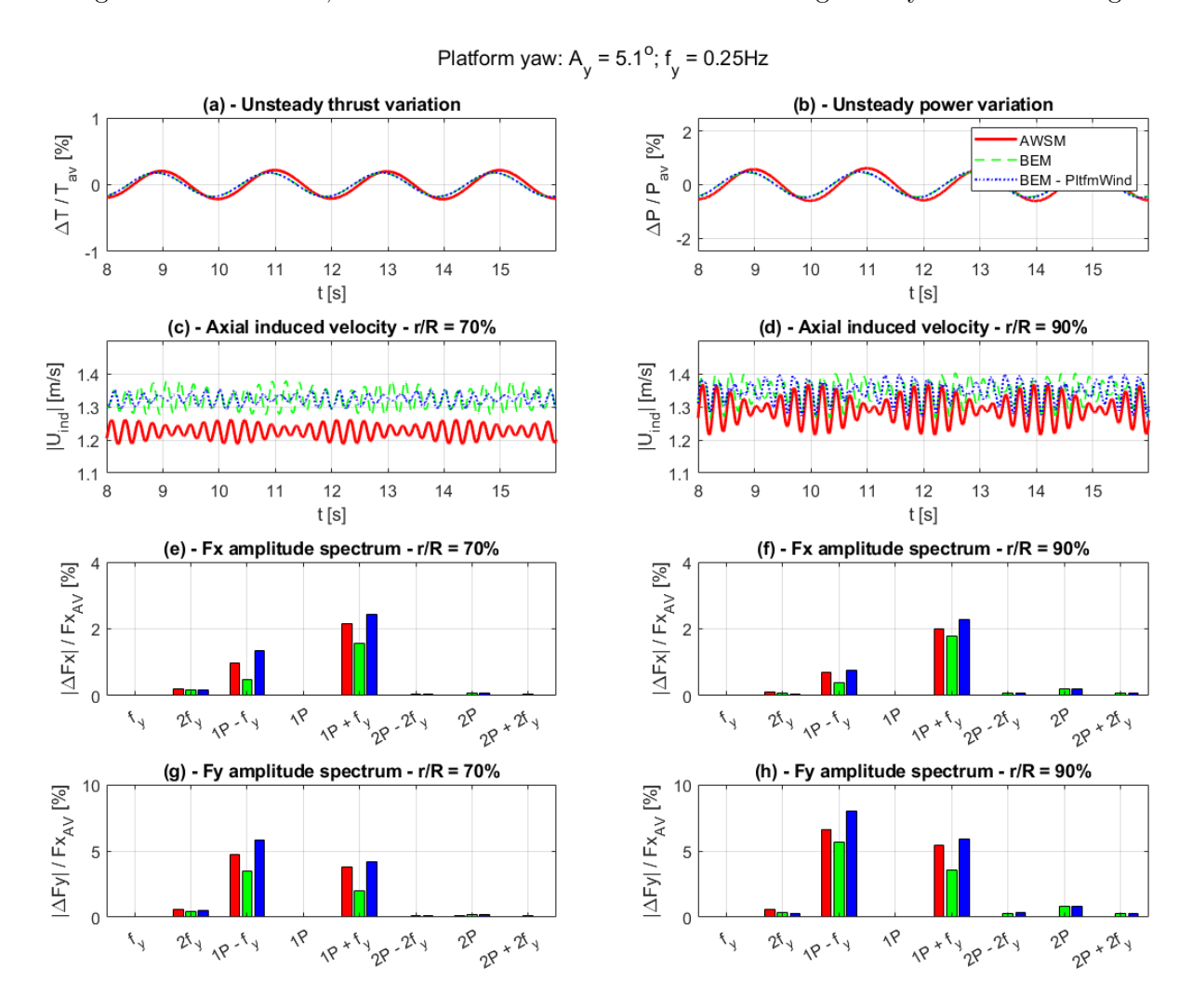


Figure 4. Platform yaw motion figures: (a) integral aerodynamic thrust variation for two yaw cycles; (b) rotor aerodynamic power variation for two yaw cycles; (c) axial induced velocity variation at 70% span for two yaw cycles; (d) Axial induced velocity variation at 90% span for two yaw cycles; (e) amplitude spectrum of the axial unit force at 70% span; (f) amplitude spectrum of the axial unit force at 90% span; (g) amplitude spectrum of the tangential unit force at 90% span.

4. New model's limitations

Despite having been tested with motions along every platform's DoF, the proposed model presents some limitations. First of all, it should not be surprising that accuracy tends to reduce as floater motions get larger. The model was indeed conceived observing that the wake behind a moving turbine affected the rotor plane quite similarly to the wake of a steady rotor immersed in a consistently varying inflow. Such an approximation becomes poorer with larger motions because the locations where wake vortices are shed get farther away from those of a steady rotor and the wake interacts differently with the rotor plane. Moreover, large motion amplitudes may

2265 (2022) 042017

doi:10.1088/1742-6596/2265/4/042017

result in the rotor entering its own wake, and this cannot be modelled with BEM. But similar conditions are very hard to model even with FVW methods because the lifting line gets very close to the vortex cores in the wake leading to unstable solutions. Overall the verification campaign has indicated that the floating BEM model improves predictions for the most common ranges of platform motions, whereas its performance has been found to be poor but not worse than the standard BEM method for the more extreme motion cases that have been tested, considering a maximum surge velocity up to $\sim 75\%$ of the free-stream wind speed.

Therefore the new model's greatest limit remains the fact that so far it has only been tested for rigid turbines, and since its main development goal is the improvement of FOWT design tools extending its validity to the flexible case has absolute priority. This is quite challenging, however, because the rigid body assumption underlying eq. 7 is only a good approximation when the first turbine natural frequency is much larger than the typical frequency range associated with platform motions, which is not true for large floating turbine rotors. Hence structural dynamic effects make $\vec{U}_{Pltfm}(P)$ much harder to estimate.

5. Conclusions and future work

An engineering model for BEM capable of simulating generic motions along each DoF of a floating platform has been presented in detail. Its results have been verified by comparing against high-fidelity FVW predictions as well as standard BEM simulations. The UNAFLOW scaled turbine [8, 26] has been modelled to maximize results reproducibility while hoping for new experimental measurements to come. A small subset of the large verification campaign conducted has been analysed considering the same imposed harmonic motion, first for the pitch and then for the yaw DoF of the floater. This comparison has provided new valuable insights on the effect of these motions on aerodynamic loads and the performance of a FOWT.

The new engineering model clearly improves BEM predictions for the pitch motion case, both in terms of aerodynamic loads and induction tracking, leading to a better agreement with the FVW results. Most of the benefit has been observed on amplitudes and phases at the motion frequency harmonic, which is the most significant for a pitching platform due to the long lever arm provided by the tower. Lacking this lever, such a peak is absent when the yaw motion is considered, resulting in less evident differences between the two BEM formulations.

Regardless of pitch or yaw, torque-generating forces have been found to be much more sensitive to the platform motion than those contributing to the thrust. Furthermore, both rotations cause similar peaks in the local aerodynamic force spectra at $1P \pm 1P$ the motion frequency. These peaks are likely associated with skewed wake effects and, occurring at relatively high frequencies, they might be quite detrimental for the fatigue life of a blade especially if they excite some system eigenmodes. In this regard, the tangential force peak at 1P plus the motion frequency might be of real concern for the first edgewise bending mode.

Because of the rotor symmetry, no trace of these high-frequency components associated with skewed wake effects has been found on the overall rotor thrust and aerodynamic power, which are completely dominated by the motion frequency harmonics in the case of platform pitch, whereas they only show small oscillations at twice the motion frequency in case of yaw. As a result, performance variations induced by the platform pitch appear one order of magnitude larger than those induced by the same yaw motion, confirming what was observed in [28].

Results of the full verification dataset (considering every single floater DoF) will be presented in a subsequent publication, hoping to include future experimental data for validation as well. In its current development stage the proposed model can only aid aerodynamic design calculations on rigid turbines since the coupling with a structural solver has not been tested yet. Therefore, the next challenging step left for future works is to test and tune this engineering model for full aero-hydro-elastic cases, so as to improve the accuracy of those loadcase calculations that will drive the design and certification of future floating wind turbine rotors.

2265 (2022) 042017

doi:10.1088/1742-6596/2265/4/042017

References

- [1] GWEC, Global offshore wind report 2021, Tech. rep., GWEC (2021).

 URL https://gwec.net/global-offshore-wind-report-2021/
- [2] H. A. Madsen, T. J. Larsen, G. R. Pirrung, A. Li, F. Zahle, Implementation of the blade element momentum model on a polar grid and its aeroelastic load impact, Wind Energy Science 5 (1) (2020) 1–27. doi:10.5194/wes-5-1-2020.
 - URL https://wes.copernicus.org/articles/5/1/2020/
- [3] D. Micallef, A. Rezaeiha, Floating offshore wind turbine aerodynamics: Trends and future challenges, Renewable and Sustainable Energy Reviews 152 (2021) 111696. doi:https://doi.org/10.1016/j.rser.2021.111696. URL https://www.sciencedirect.com/science/article/pii/S1364032121009709
- [4] T. Sebastian, M. Lackner, Characterization of the unsteady aerodynamics of offshore floating wind turbines, Wind Energy 16 (3) (2013) 339-352. arXiv:https://onlinelibrary.wiley.com/doi/pdf/10.1002/we.545, doi:https://doi.org/10.1002/we.545. URL https://onlinelibrary.wiley.com/doi/abs/10.1002/we.545
- [5] J. de Vaal, M. Hansen, T. Moan, Effect of wind turbine surge motion on rotor thrust and induced velocity, Wind Energy 17 (1) (2014) 105-121. arXiv:https://onlinelibrary.wiley.com/doi/pdf/10.1002/we.1562, doi:https://doi.org/10.1002/we.1562. URL https://onlinelibrary.wiley.com/doi/abs/10.1002/we.1562
- [6] D. Micallef, T. Sant, Loading effects on floating offshore horizontal axis wind turbines in surge motion, Renewable Energy 83 (2015) 737-748. doi:https://doi.org/10.1016/j.renene.2015.05.016. URL https://www.sciencedirect.com/science/article/pii/S0960148115003936
- [7] T. T. Tran, D.-H. Kim, A cfd study into the influence of unsteady aerodynamic interference on wind turbine surge motion, Renewable Energy 90 (2016) 204–228. doi:https://doi.org/10.1016/j.renene.2015.12.013. URL https://www.sciencedirect.com/science/article/pii/S0960148115305188
- [8] S. Mancini, K. Boorsma, M. Caboni, M. Cormier, T. Lutz, P. Schito, A. Zasso, Characterization of the unsteady aerodynamic response of a floating offshore wind turbine to surge motion, Wind Energy Science 5 (4) (2020) 1713-1730. doi:10.5194/wes-5-1713-2020. URL https://wes.copernicus.org/articles/5/1713/2020/
- [9] A. Ortolani, G. Persico, J. Drofelnik, A. Jackson, M. Campobasso, Cross-comparative analysis of loads and power of pitching floating offshore wind turbine rotors using frequency-domain navier-stokes CFD and blade element momentum theory, Journal of Physics: Conference Series 1618 (5) (2020) 052016. doi:10.1088/1742-6596/1618/5/052016. URL https://doi.org/10.1088/1742-6596/1618/5/052016
- [10] R. Kyle, Y. C. Lee, W.-G. Früh, Propeller and vortex ring state for floating offshore wind turbines during surge, Renewable Energy 155 (2020) 645-657. doi:https://doi.org/10.1016/j.renene.2020.03.105. URL https://www.sciencedirect.com/science/article/pii/S0960148120304377
- [11] K. Sivalingam, S. Martin, A. A. Singapore Wala, Numerical validation of floating offshore wind turbine scaled rotors for surge motion, Energies 11 (10) (2018). doi:10.3390/en11102578. URL https://www.mdpi.com/1996-1073/11/10/2578
- [12] C. Ferreira, W. Yu, A. Sala, A. Vire, Dynamic inflow model for a floating horizontal axis wind turbine in surge motion, Wind Energy Science Discussions 2021 (2021) 1-22. doi:10.5194/wes-2021-34. URL https://wes.copernicus.org/preprints/wes-2021-34/
- [13] K. Boorsma, M. Caboni, Numerical analysis and validation of unsteady aerodynamics for floating offshore wind turbines, Tech. Rep. TNO 2020 R11345, TNO Wind Energy, Petten, Netherlands (May 2020). URL http://publications.tno.nl/publication/34637340/MelXUe/TNO-2020-R11345.pdf
- [14] K. Boorsma, F. Grasso, J. Holierhoek, Enhanced approach for simulation of rotor aerodynamic loads, Tech. Rep. ECN-M-12-003, ECN, Petten, Netherlands (December 2011).
- [15] J. G. Schepers, Iea annex xx: dynamic inflow effects at fast pitching steps on a wind turbine placed in the nasa-ames wind tunnel, Report ECN-E-07-085, ECN (2007).
- [16] J. G. Schepers, et al., Final report of the eu project avatar: Aerodynamic modelling of 10 mw turbines, Report http://www.eera-avatar.eu/publications-results-and-links, ECN (2018).
- [17] K. Boorsma, F. Wenz, K. Lindenburg, M. Aman, M. Kloosterman, Validation and accommodation of vortex wake codes for wind turbine design load calculations, Wind Energy Science 5 (2) (2020) 699– 719. doi:10.5194/wes-5-699-2020. URL https://wes.copernicus.org/articles/5/699/2020/
- [18] J. G. Schepers, K. Boorsma, et al., Final report of iea task 29 (phase 4): detailed aerodynamics of wind turbines, Report 10.5281/zenodo.4817875, IEA Wind TCP Task 29 (2021).
- [19] A. van Garrel, Development of a wind turbine aerodynamics simulation module, Report ECN-C-03-079, ECN (2003).

2265 (2022) 042017

doi:10.1088/1742-6596/2265/4/042017

- [20] H. Snel, J. G. Schepers, Joule1: Joint investigation of dynamic inflow effects and implementation of an engineering model, Report ECN-C-94-107, ECN (1994).
- [21] G. Lloyd, Guideline for the Certification of Wind Turbines, Germanischer Lloyd, Hamburg, Germany, 2010.
- [22] F. Manwell, J. G. McGowan, A. L. Rogers, Wind Energy Explained: Theory, Design and Application, Second Edition, John Wiley and Sons, Ltd, DOI:10.1002/9781119994367, 2010.
- [23] L. Prandtl, A. Betz, Vier Abhandlungen zur hydrodynamik und aerodynamik, Selbstverlag des KaiserWilhelm-Instituts für Strömungsforschung, Göttingen, Germany, 1927.
- [24] J. G. Schepers, Engineering models in wind energy aerodynamics, development, implementation and analysis using dedicated aerodynamic measurements, Ph.D. thesis, University of Delft, Delft, Netherlands, iSBN 978-94-6191-507-8 (2012).
- [25] J. G. Schepers, L. J. Vermeer, Een engineering model voor scheefstand op basis van windtunnelmetingen, Report ECN-CX-98-070, ECN (1998).
- [26] A. Fontanella, I. Bayati, R. Mikkelsen, M. Belloli, A. Zasso, Unaflow: a holistic wind tunnel experiment about the aerodynamic response of floating wind turbines under imposed surge motion, Wind Energy Science 6 (5) (2021) 1169-1190. doi:10.5194/wes-6-1169-2021. URL https://wes.copernicus.org/articles/6/1169/2021/
- [27] H. Snel, Heuristic modelling of dynamic stall characteristics, in: Conference proceedings European Wind Energy Conference, Dublin, Ireland, 1997, pp. 429–433.
- [28] T. T. Tran, D.-H. Kim, The aerodynamic interference effects of a floating offshore wind turbine experiencing platform pitching and yawing motions, Journal of Mechanical Science and Technology 29 (2014) 549–561. doi:https://doi.org/10.1007/s12206-015-0115-0.